J Appl Electrochem (2014) 44:5–22
DOI 10.1007/s10800-013-0620-8

REVIEW PAPER

A review of high energy density lithium–air battery technology

Md. Arafat Rahman · Xiaojian Wang · Cuie Wen

Received: 20 June 2013 / Accepted: 18 August 2013 / Published online: 29 August 2013

Abstract Today's lithium (Li)-ion batteries have been widely adopted as the power of choice for small electronic devices through to large power systems such as hybrid electric vehicles (HEVs) or electric vehicles (EVs). However, it falls short of meeting the demands of new markets in these areas of EVs or HEVs due to insufficient energy density. Therefore, new battery systems such as Li–air batteries with high theoretical specific energy are being intensively investigated, as this technology could potentially make long-range EVs widely affordable. So far, Li–air battery technology is still in its infancy and will require significant research efforts. This review provides a comprehensive overview of the fundamentals of Li–air batteries, with an emphasis on the recent progress of various elements, such as lithium metal anode, cathode, electrolytes, and catalysts. Firstly, it covers the various types of air cathode used, such as the air cathode based on carbon, the carbon nanotube-based cathode, and the graphene-based cathode. Secondly, different types of catalysts such as metal oxide- and composite-based catalysts, carbon- and graphene-based catalysts, and precious metal alloy-based catalysts are elaborated. The challenges and recent developments on electrolytes and lithium metal anode are then summarized. Finally, a summary of future research directions in the field of lithium air batteries is provided.

Keywords Energy density · Lithium · Anode · Cathode · Catalyst · Electrolyte

Md. A. Rahman · X. Wang · C. Wen (✉)
Faculty of Engineering and Industrial Science, Swinburne University of Technology, Hawthorn, VIC 3122, Australia
e-mail: cwen@swin.edu.au

1 Introduction

Energy is the indispensable part of modern society. Recently, global warming, diminishing fossil-fuel supplies, and environmental pollution have driven the increasing usage of renewable energy. However, the supply of renewable energy fluctuates with time and the season of the year. The development of novel energy storage and conversion system is required for effective utilization of renewable energy sources in future smart grids and power delivery systems. Numerous energy storage systems, such as mechanical, magnetic, chemical, and electrochemical, are currently being investigated [1]. Among them, one of the most attractive systems is electrochemical storage process, which converts chemical energy into electrical energy by sharing a common carrier electron [2]. Batteries and fuel cells are among the electrochemical storage devises that ensure such conversions to occur in a reversible or a single way.

The Li-ion battery is the best performing among the present batteries, owing to its energy density of 210 Wh kg^{-1} or 650 Wh L^{-1} [3]. The Li-ion battery captured both the portable electronic market and the power tool equipment market because of attractive performances in areas such as its long life cycle and rate capability [4]. Most of today's EVs, especially cars, use Li-ion batteries for propulsion. However, Li-ion battery-powered EVs are limited to a driving range of 160 km on a single charge, and the cost of the battery itself accounts for nearly 65 % of the total cost of car [5, 6]. Recently, the Li–air battery was proposed as the most promising candidate to power electric cars, as it could deliver 5–10 times greater energy density than the current lithium-ion batteries. The theoretical specific energy density of a Li–air battery is 5,200 Wh kg^{-1} (by taking into consideration the mass of

lithium anode and the oxygen (O_2) gained during discharge), as compared to a Li-ion which is 150 Wh kg^{-1} [7]. In theory, the energy density can be compared to that of a gasoline engine (13,000 Wh kg^{-1}, where the practical energy density is 1,700 Wh kg^{-1}) [8]. However, this conception is in debate due to inflated specific energy density of Li–air battery based on the anode mass and O_2 by ignoring cathode, electrolyte, and other cell components. Theoretical gravimetric and volumetric energy densities using aqueous electrolytes have been investigated based on Li metal anode, air electrode, and electrolyte [9]. It has been determined that the maximum theoretical gravimetric and volumetric energy densities are 1,300 Wh kg^{-1} and 1,520 Wh L^{-1} in basic electrolyte, and 1,400 Wh kg^{-1} and 1,680 Wh L^{-1} in acidic electrolyte, respectively. There are several scientific/technical hurdles that must be overcome in order to design a rechargeable Li–air battery, such as the incomplete discharge as porous carbon cathode, which blocks discharge products, the unstable cathode in atmospheric moisture [10], an inadequate understanding of the catalytic effect [11], the higher charge overpotential in comparison with the discharge overpotential [12], the decomposition of carbonate-based electrolytes during discharge, and the formation of alkyl carbonates. Li_2CO_3 [13] and Li_xO_y (Li_2O_2 or Li_2O) are the preferred discharge products formed during O_2 reduction in nonaqueous electrolytes, although severely affects (Li_2O is not oxidizable during charging [13]) the rechargeability and life cycle of the battery [14]. However, the practical feasibility of a rechargeable Li–air battery with organic electrolyte has been investigated by Abraham and Jing [15]. The cell was cycled several times and the obtained capacity was about 1,300 mAh g_c^{-1}. The reduction product at the cathode is Li_2O_2, although formation of Li_2O may be favoured at high discharge rates [16]. The possible cathodic mechanism could involve the following reactions that are generally referred as oxygen reduction reaction (ORR):

$$O_2 + Li^+ + e^- \rightarrow LiO_2\,(3\,V\ vs.\ Li/Li^+) \quad (1)$$

$$2LiO_2 \rightarrow Li_2O_2 + O_2 \quad (2)$$

$$LiO_2 + Li^+ + e^- \rightarrow Li_2O_2\,(3.1\,V\,vs.\ Li/Li^+). \quad (3)$$

The electrochemical decomposition of Li_2O_2 to Li and O_2 on charging has been demonstrated by Ogasawara et al. [17], and the corresponding oxygen evolution reaction (OER) is

$$Li_2O_2 \rightarrow 2Li^+ + 2e^- + O_2. \quad (4)$$

The pathways followed on O_2 reduction and evolution reactions are different. An in situ spectroscopic study of O_2 reaction in aprotic electrolyte by Peng et al. [18] showed that LiO_2 is an intermediate species during O_2 reduction before the final product Li_2O_2. However, Li_2O_2 decomposes directly in one-step reaction to evolve O_2 and does not produce LiO_2 as an intermediate product. It has been demonstrated that the formation of the discharge products (Li_2O_2 or LiO_2) strongly depends on the kinetic of ORR, which is affected by the presence of various catalyst [19] and as well as by the type of electrolytes and solvents [20] used in the Li–air batteries. In addition, in situ transmission electron microscopic observations of electrochemical oxidation of Li_2O_2 are reported by Zhong et al. [21]. In this study, oxidation of electrochemically formed Li_2O_2 particles, supported on multiwall carbon nanotubes (MWCNTs), was found to occur preferentially at the MWCNTs/Li_2O_2 interface and suggested that electron transport in Li_2O_2 ultimately limits the oxidation kinetics at high overpotential. These are the few mechanisms of O_2 reduction and evolution reaction for Li–air batteries. The field of Li–air batteries is currently undergoing exciting development, with increasing achievements. This review paper summarizes the recent developments of rechargeable Li–air batteries, including air cathodes, catalysts, electrolytes, and lithium metal anodes, with the aim of providing a better understanding of this technology.

2 Recent breakthroughs in lithium–air battery elements

There are four types of Li–air batteries, when defining on the basis of the electrolyte used, as shown in Fig. 1: (1) aqueous electrolytic type, (2) aprotic/nonaqueous electrolytic type, (3) mixed/hybrid electrolytic type, and (4) solid-state electrolytic type. All the four types of Li–air batteries use Li metal as the anode and O_2 gas as the cathode. The air electrode of these cells consists of a carbon matrix with a catalyst, which serves as the host structure for the reversible formation of Li_2O_2 according to the reaction:

$$2Li^+ + 2e^- + O_2 \rightarrow Li_2O_2.$$

A liquid organic electrolyte is used in aprotic/nonaqueous electrolytic type of Li–air batteries. Lithium salts such as $LiPF_6$, $LiAsF_6$, $LiN(SO_2CF_3)_2$, and $LiSO_3CF_3$ in organic solvent such as organic carbonates, ethers, and esters are commonly used electrolytes [22]. The configuration of the aqueous electrolytic type of Li–air battery is similar to that of aprotic type except that the electrolyte used is aqueous based. However, in aprotic electrolyte, the specific capacity of the aprotic-type Li–air battery is limited by the precipitation of lithium oxides within the pores of carbon cathode and solubility of O_2 in the electrolyte solution, which affect the transport of O_2 within the interior of the air cathode [23]. In contrast, the aqueous Li–air battery avoids the issue of cathode clogging because the

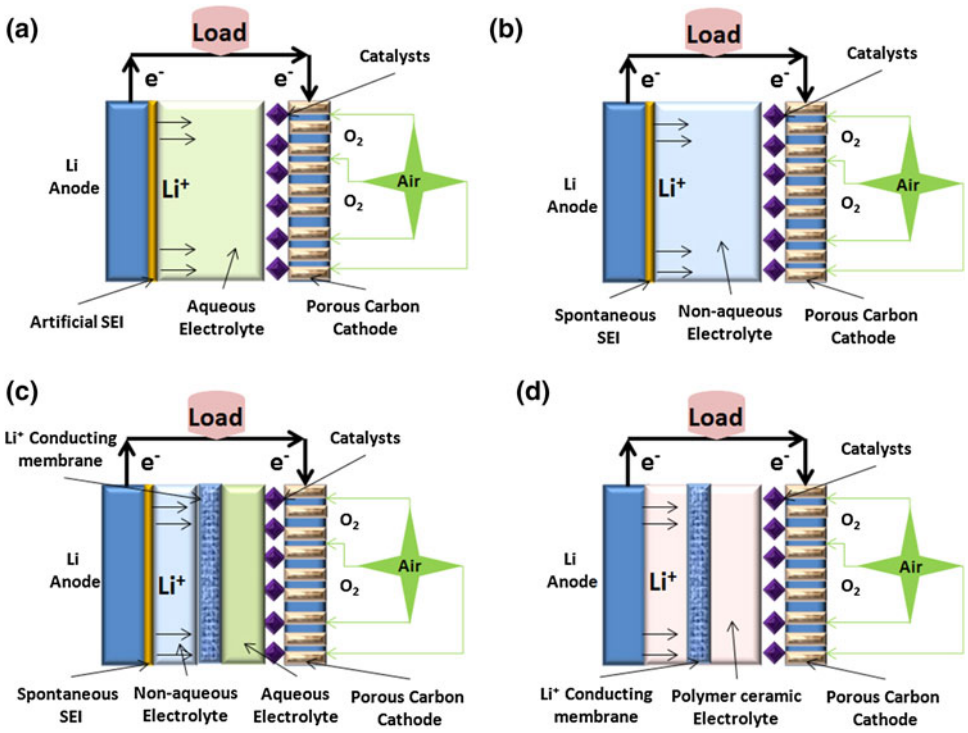

Fig. 1 Types of lithium–air batteries: **a** Aqueous electrolytic type, **b** aprotic/nonaqueous electrolytic type, **c** mixed (aprotic-aqueous) type, and **d** solid-state type

reaction products are water soluble, which allows aqueous Li–air batteries to maintain performance over time [24]. However, lithium as an anode reacts violently with water, and thus, the aqueous Li–air battery requires an artificial solid electrolytic interface (SEI). Usually, a lithium ion-conducting glass or ceramic is used as SEI [24]. Both aprotic- and aqueous-type electrolytes are used in the mixed type of Li–air battery to overcome limitations of the aqueous-type or the aprotic-type Li–air battery. A lithium metal anode is in contact with the aprotic side while the porous carbon cathode is in contact with the aqueous side. Usually, a lithium ion-conducting ceramic is used as the membrane joining the two electrolytes [24]. Rechargeable solid-state Li–air battery is composed of solid electrolyte [25]. However, the main drawback of this type of battery is lower ionic conductivity of the glass–ceramic electrolytes such as NASICON structure of $Li_{1+x}Ge_{2-x}Al(PO_4)_3$ electrolyte compared to liquid electrolytes [26]. The ultimate choice for the best configuration is still a technical issue because each configuration of these Li–air batteries has inimitable merits and shows definite scientific challenges. A preview of some of these issues is given bellow.

2.1 Air cathode

The most common air cathode is composed of a porous carbon, a catalyst, and a polymer binder to hold the catalyst on the cathode. To date, the main challenges for the air cathodes are as follows:

1. The design and synthesis of a novel porous carbon material with high conductivity. It should provide sufficient pores to store the discharge products and channels for O_2 diffusion. It also should have good electrolyte wettability, ensuring an adequate and suitable three-phase interface for the charge/discharge process [27].
2. Prevention of corrosion of the catalyst, which is considered to be the result of the oxidation of carbon [28].
3. Prevention of the ingression of H_2O and CO_2 into the cell [14].

The performance of the Li–air battery is determined substantially by the air cathode [10]. The cathode reactions not only deliver most of the cell voltage, but most of the cell voltage drop also occurs at the cathode. Figure 2 presents the voltage distribution of Li–air battery and the structure of a porous carbon cathode [29]. In the case of Li–air batteries, Li^+ goes through the electrolyte to the air cathode and forms Li_2O_2 precipitate. The pores of the cathode are densely filled by the Li_2O_2 precipitate as discharge occurs, which prohibits the ORR as O_2 comes through the pores of the carbon cathode from the ambient atmosphere. In addition, Li_2O_2 also affects the volumetric and specific energy densities. For instance, in the case of a Li–air battery, assuming O_2 is free

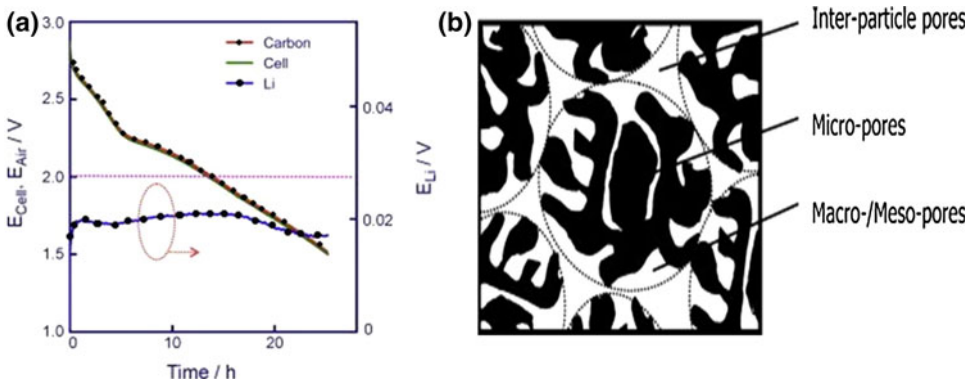

Fig. 2 **a** The potential distribution of a lithium anode (*right vertical axes* and *curve is circled*) and an air cathode (*left vertical axes* very close to overall cell potential), **b** model of porous carbon electrode for lithium–air battery (adapted from [29])

and the nominal potential of the battery is 3 V, the specific energy can be calculated by:

$$\text{Specific energy} = \left(3\ \text{V} \times 96{,}500\ \text{C Mole}^{-1}\right)/ \left(3{,}600\ \text{C Ah}^{-1} \times 0.0069\ \text{kg mol}^{-1}\right) = 11{,}640\ \text{Wh kg}^{-1}$$

where the atomic weight of lithium is 6.9 g/mol, and similarly, the gravimetric energy density of Li_2O_2 (peroxide) is 3,500 Wh kg^{-1}, meaning that the current volumetric energy density is <20 % of the theoretical values [30]. In the ideal case, peroxide (Li_2O_2) and oxide (Li_2O) are expected to decompose during discharge by ORR and charge by OER.

2.1.1 Air cathode based on carbon

The microstructure of a porous carbon cathode is a major factor in the performance and life cycle of Li–air batteries. Various carbon materials, such as carbon powders, mesoporous carbon, carbon nanotubes and fibers, and graphene, have been used as the air electrodes for Li–air batteries. It has been shown that the uniformity of the pore size plays an important role in determining the electrochemical performance [31, 32]. The large volume expansion in the Ketjen black (KB)-based electrode led to extra triphase regions, able to facilitate the reaction in the electrode, and extra volume to hold the reaction product. Consequently, a Li–air battery assembled using KB-based air electrode exhibited the highest specific capacity of 851 mAh g^{-1}. Furthermore, carbons with ordered and interconnected mesopores can be used as an efficient catalyst support that provides inner pores for gas diffusion and outer surfaces for electrolyte access [33]. In addition, for a Li–air battery, an interconnected dual pore system with a multiple time-release catalyst has been proposed in order to increase the materials utilization, to decrease diffusion limitation, and to supply high power for long periods of time [34]. The specific capacity can be optimized by the use of a carbon microstructure and loading as well as the porosity or thickness of the electrodes and the amount of electrolyte [31]. Therefore, large and thin electrodes tightly wound into cylindrical cells or folded into prismatic cells cannot be used, since they would lead to air starvation. Moisture and CO_2 in atmospheric air should be separated from O_2 since the lithium electrode needs to be protected from moisture in air. In these circumstances, the specific surface area has positive effects on a specific capacity [35]. The specific capacity is proportional to the surface area of the air cathode because it facilitates an electrochemical reaction for the formation of lithium oxide. The high surface area results in the more specific capacity of the batteries [36]. It has been shown that an appropriate pore size is very important in regard to high specific capacity. If the entrances of the pores are too small, such as with micropores, the pores can easily be blocked by lithium oxide dendrites and restrict the full use of pore surfaces. Compared to commercial carbon powder materials, mesostructured materials, such as mesocelluar carbon foam (MCF-C), have larger mesopores and are beneficial for accommodating discharge products [37]. Similar results have also been reached according to other reports, using mesoporous carbon aerogels with tunable porosity through the polycondensation of resorcinol with formaldehyde [38]. The discharge capacity of the porous carbon showed that appropriate pore volume and pore diameters are the key factors in achieving high capacity. Furthermore, comparing discharge characteristics of Li–air batteries with different carbon cathodes has been revealed that mesopore volume of carbon materials has large contribution to the capacity [39]. Therefore, the employment of carbon nanostructures with optimized morphologies and textures may offer great opportunity to attain high-performance Li–air batteries. However, the oxidation of carbon is a serious problem, especially at high voltage during charge, for the long-term stability of the air cathode. Arai et al. [40] investigated the KB electrode surface area of 1,300 $m^2\ g^{-1}$ for ORR and OER in aqueous 8 M KOH solution. It is reported that the electrode deterioration during OER claimed that the degradation resulted in a loss of the electrochemically active surface area of electrode, mainly due to carbon corrosion.

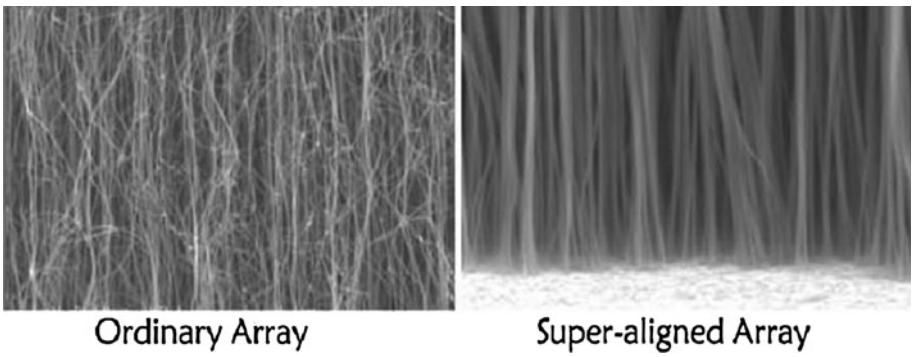

Fig. 3 Comparison of ordinary arrays and super-aligned arrays of carbon nanotubes (adapted from [45])

Recently, Bruce et al. [41] also reported that carbon is more unstable upon charging above 3.5 V versus Li/Li^+ in aprotic electrolyte, and upon discharge, there is little or no decomposition of hydrophobic carbon, whereas some decomposition does occur for hydrophilic carbon. In addition, it is reported that direct chemical reaction with Li_2O_2 is not primarily responsible for carbon corrosion, and as carbon decomposition is much less at or below 3.5 V, carbon may be a suitable electrode if charging of Li_2O_2 could be carried out below 3.5 V [41]. More recently, the air electrode performance of various carbon materials, such as KB, acetylene black (AB and AB-S), Vulcan XC-72R (VX), and vapor grown carbon fiber (VGCF), has been investigated [42]. In this study, the gas in the cells with the KB, VX, and AB-S electrodes was analyzed, and hydrogen and CO were observed for the OER. The molar ratio of hydrogen to CO was approximately 10. It has been claimed that the CO gas may come from the carbon electrode, because there was no carbon source in the cell, except the carbon in the electrode. However, the carbon electrode performance for OER was improved, and the amount of CO was significantly decreased by the addition of catalyst [42]. Therefore, the oxidation of carbon is a serious problem for the long-term stability of the air cathode. A more stable catalyst for the OER and ORR, especially for the OER, should be developed for the air cathode with a lower overpotential at a high current density.

2.1.2 Air cathode-based carbon nanotube (CNT)

Materials with proper nanoscale dimensions and architectures have the potential to dramatically enhance the transport of electrons, ions, and the molecules associated with the cycling of batteries, significantly accelerating the rate of the chemical and transportation processes [43]. CNT and carbon nanofibers (CNFs) have been widely studied to enhance the electrochemical performance in a lithium–air battery. For instance, aligned CNFs electrodes were fabricated using atmospheric pressure chemical vapor deposition (CVD) [44]. The CNFs electrodes showed unique properties such as a high void volume, high electronic conductivity, and an interconnected porous structure that plays a significant role in determining battery performance. Furthermore, super-aligned CNT arrays, films, and yarns have been synthesized, which exhibit high nucleation density and narrow size distribution of catalysts [45]. Thus, high surface catalyst density and a narrow CNT diameter are the key features of super-aligned CNT arrays, as shown in Fig. 3.

Doping of carbon with nitrogen atoms has attracted a lot of attention because conjugation between the nitrogen lone-pair electrons and graphene π-systems may create nanostructures with desired properties such as improved ORR activity [46–48]. Recent studies indicated that nitrogen functionality on carbon is responsible for the electrocatalytic activity of a cathode, enhancing the cell capacity of a Li–air battery [49–51]. A comparison study has been carried out on pristine CNTs and nitrogen-doped carbon nanotubes (N-CNTs) as cathode materials in aprotic Li–air batteries and is shown in Fig. 4 [52].

Nitrogen-doped carbon nanotubes showed a typical bamboo-like structure, which indicates that nitrogen atoms were introduced into the carbon structure. Accordingly, the diameter of N-CNTs increased to 50–60 nm compared to 40–50 nm before doping. The N-CNTs showed a lower average charging plateau voltage (4.22 V) and a higher capacity (630 mAh g^{-1} of Li_2O_2) than CNTs. These results revealed that the N-CNTs were more efficient for Li_2O_2 decomposition, indicating a high catalytic activity in the charge process. In addition, the N-CNTs electrode delivered an initial discharge capacity of 866 mAh g^{-1}, which is about 1.5 times that of the CNTs electrode (596 mAh g^{-1}).

2.1.3 Air cathode based on graphene

Graphene nanosheets (GNSs), which have a two-dimensional carbon nanostructure, have attracted a great deal of attention for Li–air battery applications due to their superior properties, such as high thermal conductivity ($\sim$5,000 W m^{-1} K^{-1}), high electric conductivity (10^3–10^4 S m^{-1}), and high specific surface area (2,630 m^2 g^{-1})

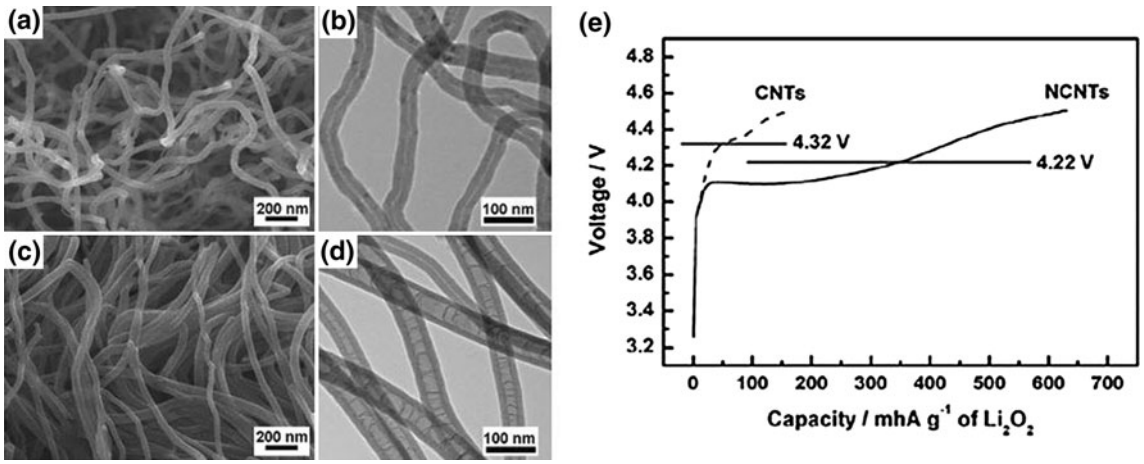

Fig. 4 **a** SEM image of CNTs, **b** TEM image of CNTs, **c** SEM image of N-CNTs, **d** TEM image of N-CNTs, **e** variation of voltages on charging cells with CNTs and N-CNTs electrodes at a density of 75 mA g^{-1} (adapted from [52])

[28]. A novel air electrode consisting of a hierarchical arrangement of functionalized graphene sheets (FGS) with no catalysts was fabricated by a colloidal microemulsion approach, as shown in Fig. 5 [53]. This 3D structure consisted of interconnected pore channels on both the micormeter and nanometer length scales and revealed an extremely high capacity of 15,000 mAh g^{-1}.

Graphene nanosheets with a thin, wrinkled structure prepared by the oxidation of graphite powder using modified Hummer's method delivered a capacity of 8,707.9 mAh g^{-1}, due to its unique morphology and structure [54]. This electrode increased the electrochemically accessible site and provided a larger diffusion path for O_2, thereby significantly improving the discharge capacity. After discharging, the Li_2O_2 was observed on both sides, as well as at the edges of the GNSs after discharge. GNSs electrodes exhibited a much better cycling stability and lower overpotential (1.22 V) than that of the Vulcan XC-72 carbon (1.66 V) on the third cycle per gram of carbon in the electrode as shown in Fig. 6a [55]. The cycling performance of GNSs and the Vulcan carbon (VC) electrodes is shown in Fig. 6b. The initial capacity of the GNSs electrode was 1,597 mAh g^{-1} and then dramatically increased to 2,332 mAh g^{-1} on the second cycle and was finally sustained at 2,359 mAh g^{-1} on the fifth cycle, while for the Vulcan XC-72 carbon electrode, the initial capacity was 1,918 mAh g^{-1} and it steadily declined to 1,342 mAh g^{-1} until the fifth cycle.

Nitrogen-doped graphene nanosheets (N-GNSs) and sulfur-doped graphene nanosheets (S-GNSs) as cathode material of Li–air battery have been investigated [56, 57]. It was found that the morphology of discharge product in S-GNSs cathode was significantly different from the pristine GNSs cathode with improved charging performance [57]. The morphology and distribution of discharge products of Li_2O_2 is critical to further catalytic effects, affecting the performance of battery. It is important to design optimal growth of Li_2O_2 via substrate control and therefore improve the discharge and charge properties of the battery.

2.2 Catalyst

The lithium–air battery has been the subject of intense research interest for its high energy density capacity but the voltage gap between discharge and charge is usually higher

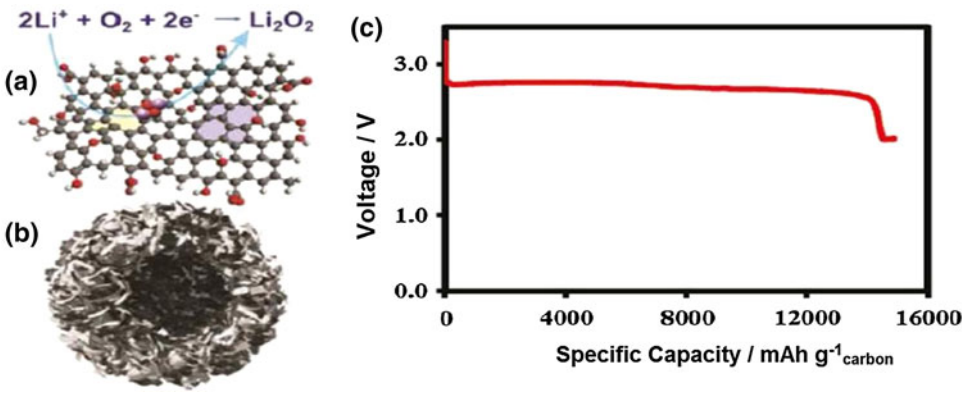

Fig. 5 Schematic structure of a functionalized graphene sheet: **a** with an ideal bimodal porous structure, **b** using FGS (C/O = 14) as the air electrode (P_{O2} = 2 atm), **c** the discharge curve of lithium–air battery (adapted from [53])

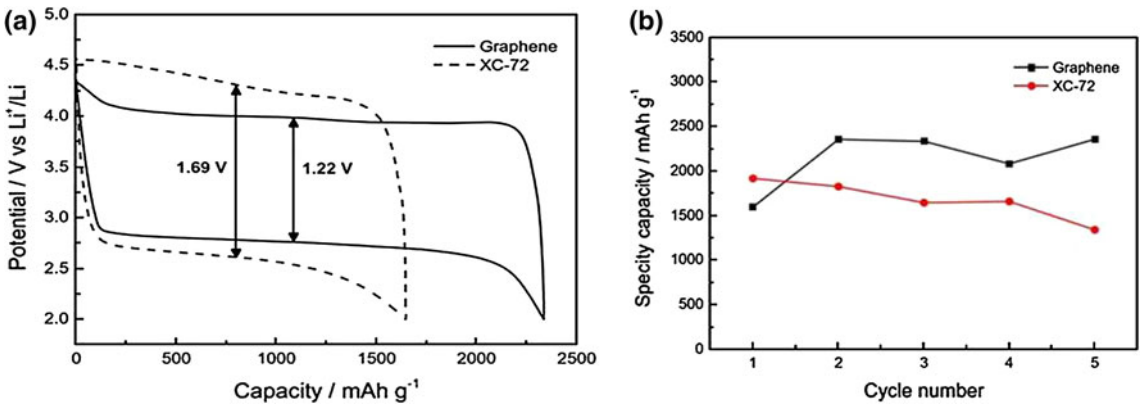

Fig. 6 Performances of GNSs and Vulcan XC-72 carbon electrode: **a** charge/discharge voltage profiles (third cycle) and **b** cycling performances at a current density of 50 mA g^{-1} (0.1 mA cm^{-2}) in 1 atm. O_2 atmosphere (adapted from [55])

than 1 V. Thus, the round-trip efficiency is significantly lower than that of the lithium–ion battery. Electrocatalysts can reduce the overpotential of discharge/charge reactions and thus increase the round-trip efficiency and improve the cycle performance [43]. It is also reasonable to assume that electrocatalysts also play an important role in ORR and OER, and hence improve the kinetics and efficiency of the Li–air battery [58, 59]. Therefore, great effort has been devoted to designing and developing novel electrocatalysts. There are a number of categories of electrocatalysts reported in the literature.

2.2.1 *Metal oxides and their composites*

An investigation of ORR and OER in nonaqueous (and aqueous) Li–air cells, using metal oxide catalysts, has been undertaken [58]. Li–air cells with bismuth and lead oxide catalysts (BiRO, PbRO) exhibit an indexed higher capacity in every cycle. The discharge capacities on the third cycle are even higher, and in the case of BiRO, the capacity reaches a maximum value of 10,000 mAh g^{-1}. In addition, a Li–air battery with a composite α-MnO_2 catalyst/CNT cathode displayed a significant rechargeability as compared to that without catalyst. In summary, α-MnO_2 reacts with the discharge product Li_2O to form Li_2MnO_3 during discharge and Li_2O is electrochemically removed from the $LiMnO_3$ during charge. This composite cathode enhanced the charge process and displayed significant capacity, when charging with catalysts (>10,000 mAh g^{-1}) and without catalysts (>4,000 mAh g^{-1}), as shown in Fig. 7 [60]. However, another observation made regarding the charge and discharge processes was that even with the α-MnO_2 catalyst, the cyclability of Li–air cell was very limited and the recharge capacity decreased within the first ten cycles.

It has been reported that the ORR and OER can take place even in the absence of a catalyst [61]. In this study, materials such as Pt, $La_{0.8}Sr_{0.2}$ MnO_3,Fe_2O_3, NiO, Fe_3O_4,

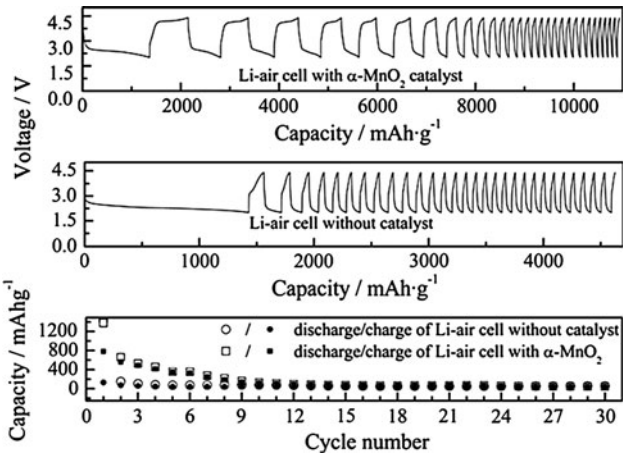

Fig. 7 Discharge/charge cycle performance of lithium–air battery with and without α-MnO_2 catalyst (at a constant current density 0.2 mA cm^{-2}) (adapted from [60])

Co_3O_4, CuO, and $CoFe_2O_4$ (1–5 μm) were investigated as catalysts. Co_3O_4 showed the lowest voltage for OER as 4.0 V, the first discharge capacity around 2,000 mAh g^{-1}, and capacity retention on cycling. In contrast, the Fe_2O_3 catalyst showed the highest first discharge capacity around 2,700 mAh g^{-1}, whereas Fe_3O_4, CuO, and $CoFe_2O_4$ catalysts exhibited the most stable cycle performance. Table 1 shows a comparison of the electrochemical performances of these catalysts.

In addition, the morphology and phase of a catalyst can significantly affect its performances. As an example, α-MnO_2, β-MnO_2, λ-MnO_2, electrolytic manganese oxide (EMD), Mn_2O_3, and Mn_3O_4 were also investigated as catalysts and α-MnO_2 nanowires exhibited the best performance, delivering about 3,000 mAh g^{-1} at a current density of 75 mA g^{-1}, showing a stable cycle performance for 10 cycles, as shown in Fig. 8 [62]. Therefore, it is evident that the α-MnO_2 nanowires are the more effective catalysts than the bulk α-MnO_2 materials.

Table 1 Discharge voltage and discharge capacities at cycles 1, 5, and 10 of cathodes with various catalysts (Adapted from [61])

Catalyst	Discharge voltage/V	Capacity of cycle 1/mAh g^{-1}	Capacity of cycle 5/mAh g^{-1}	Capacity of cycle 10/mAh g^{-1}
Pt	2.55	470	60	60
$La_{0.8}Sr_{0.2}MnO_3$	2.6	750	75	40
Fe_2O_3	2.6	2700	500	75
Fe_2O_3-carbon loaded	2.6	2500	280	75
NiO	2.6	1600	900	600
Fe_3O_4	2.6	1200	1200	800
Co_3O_4	2.6	2000	1900	1300
CuO	2.6	900	900	600
$CoFe_2O_4$	2.6	1200	900	800

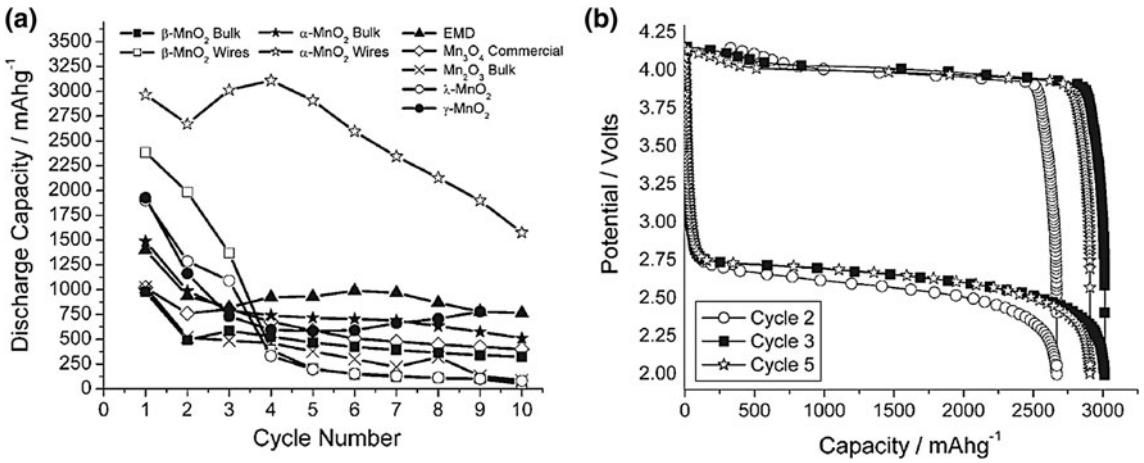

Fig. 8 **a** Discharge capacity versus cycle number for several porous electrodes containing manganese oxides as catalysts, **b** potential versus state of charge for a porous electrode containing α-MnO_2 nanowires (adapted from [62])

In contrast, transition metal-N_4 macrocycles such as iron and cobalt phthalocyanines (FePc, CoPc) have attracted considerable attention as alternative to the precious metal cathode catalysts, due to their activity and selectivity toward the ORR [63]. Li–air batteries with CoPc on mesoporous carbon have been investigated [64]. The cathode carbon/CoPc showed a larger capacity of 2,220 mAh g^{-1} at the discharge rate of 0.1 mA cm^{-2} and a slightly greater capacity of 2,430 mAh g^{-1} at the discharge rate of 0.01 mA cm^{-2}. In contrast, aprotic Li–air cell with heat-treated FeCuPc complexes as the catalyst on Ketjenblack EC-600JD has been investigated for O_2 reduction [65]. The Li–air batteries with FeCu/C showed at least 0.2 V higher discharge voltage at 0.2 mA cm^{-2} than those with pristine carbon, and it is attributed to the reduced polarization by FeCu/C catalyst.

2.2.2 *Carbon matrix and graphene*

Carbon can function as both a substrate (for electrocatalysts) and catalytic active material toward the ORR through a $2e^-$ pathway. It is worthy mentioning that carbon with defects or dopants improves ORR kinetics in aqueous solution. In addition, carbon nanostructures can serve not only as catalyst support but also as catalytically active components themselves because of different electrochemical properties to traditional bulk carbon forms. Periodic density functional theory (PDFT) implies that the edge structure of carbon is involved in ORR activity by lowering the O_2 adsorption barrier and electron transfer [66]. The electrocatalytic performance of composite electrodes Mn_3O_4/mesoporous carbon (CMK-3), Mn_3O_4/activated carbon (AC), and Mn_3O_4/MWNTs for ORR has been investigated [33]. Mn_3O_4 nanoparticles were artificially loaded on the outer surface of CMK-3 to create effective gas diffusion channels, thus ensuring sufficient three-phase interface area for electrocatalytic reaction. In addition, due to the unique structure of Mn_3O_4/CMK-3 shown in Fig. 9, the result of electrochemical testing indicated that Mn_3O_4/CMK-3 composites for ORR were much higher activity than those of other carbon-based composite catalysts (Mn_3O_4/AC and Mn_3O_4/MWNTs) [33].

Nickel cobalt oxide ($NiCoO_4$) nanostructures on graphene as an active bifunctional electrocatalyst has been

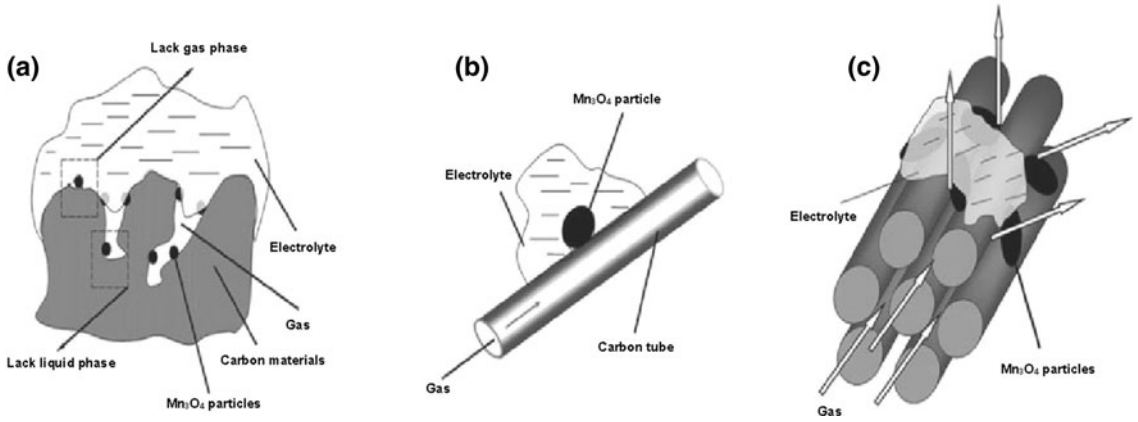

Fig. 9 Schematic view of the structure of different carbon matrix-based catalysts: **a** Mn_3O_4/AC, **b** Mn_3O_4/MWNTs, and **c** Mn_3O_4/CMK-3 (adapted from [33])

investigated [67]. Graphene with a nonprecious metal oxide, such as $NiCoO_4$, has been used to produce bifunctional electrocatalysts. A significant improvement in the polarization during ORR with $NiCo_2O_4$/graphene and current density during OER over $NiCo_2O_4$ alone was observed [67]. In addition, tetragonal $CoMn_2O_4$ (CMO) spinel nanoparticles were grown over the surface of graphene sheets (CMOG) and the performance of CMOG over ORR and OER using a rotating-disk setup was studied [68]. It should be noted that graphene oxide without a catalyst exhibits activity for the ORR that is only slightly higher than that of glassy carbon (GC). When the current of the CMOG cathode reached -0.1 mA, the CMOG cathode showed a potential of 220 mV, which is higher than that of graphene sheets, but it is 90 mV lower than that of a standard cathode of 20 wt% Pt on 80 wt% XC-72. Interestingly, at a potential of −1.0 V, the current of the CMOG cathode is about four times higher than that of graphene sheets and GC, as shown in Fig. 10a. However, compared to the bare glassy carbon electrode, the onset potential was 50 mV lower while the current of CMOG at 0.5 V was more than five times higher as shown in Fig. 10b, which indicates that the OER activity led to less polarization while Li–air battery was charged.

A nitrogen-doped graphene-rich nanocomposite with controllable morphology catalysts, as shown in Fig. 11a, has been investigated [69]. This graphene-rich catalyst exhibited much improved ORR activity and cathode performance with the addition of Co in the nonaqueous electrolyte in a lithium–air battery, relative to the currently used carbon- and Pt-based catalysts [69]. The resulting Co-based catalysts exhibited superior performance compared to Pt catalysts, reflected by a positive difference in the ORR half-wave potential, $E_{1/2}$ (2.42 V for Pt vs. 2.77 V for Co–N–MWNTs (Fig. 11b) and, to a lesser degree, by a difference in the onset potential (3.0 V for Pt vs. 3.1 V for Co–N–MWNTs (Fig. 11c).

2.2.3 *Precious metals alloy*

An important breakthrough in the improvement of the charging efficiency of Li–air batteries was the finding that gold (Au) can enhance the ORR during discharge and Pt can facilitate OER during charge. Lu et al. [11] reported that ORR and OER require different catalysts due to their different catalytic mechanisms. For instance, platinum (Pt) is a much better catalyst for OER but gold (Au) is excellent for ORR. PtAu nanoparticles (6–7 nm in diameter) were used as the catalyst on a carbon cathode [70]. The PtAu catalyst exhibited ORR at 2.7 V and OER at 3.6 V comparable to those of Au 2.7 V and Pt 3.6 V catalysts separately when the current density was 100 mA g^{-1}, as shown in Fig. 12 [70]. This indicates that the surface Pt and Au atoms on PtAu/C were responsible for the OER and ORR kinetics, respectively. It is also notable that the PtAu catalyst exhibited lower OER potentials than metal oxide catalysts such as α-MnO_2 and Co_3O_4. Li–air batteries built with a PtAu catalyst boasted the highest cell efficiency for a Li–air cell, with a round-trip efficiency of 77 % [70].

Nonprecious metals or less noble metal such as palladium (Pd), silver (Ag), and their composites have also been the subject of many investigations because of their modest activity and relatively higher abundance [71–73]. In particular, Ag shows sensibly activity and stability with a price only about 1 % of Pt, representing an attractive ORR catalyst [74]. However, Ag is relatively less stable and less electrocatalytically active in acidic media compared to Pt. Furthermore, studies have shown that porous Ag membranes provide electrocatalytic function with high exchange current density, mechanical support, and a means of current

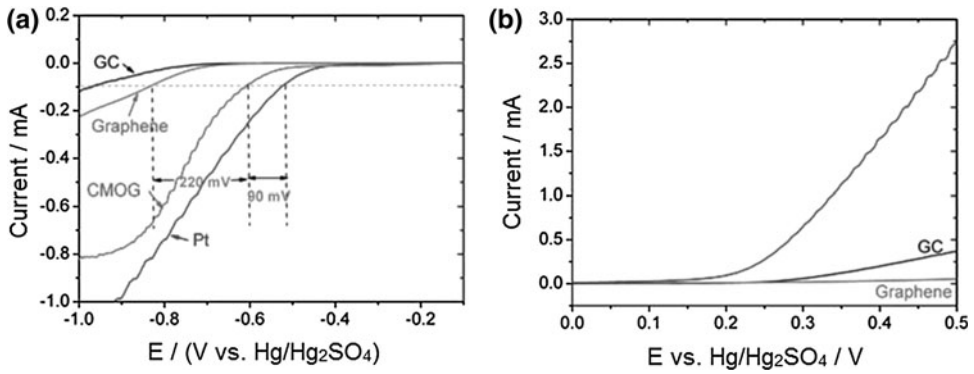

Fig. 10 Comparison of **a** ORR polarization curves of a GC electrode, 20 wt% Pt on 80 wt% XC-72, and CMOG, **b** OER polarization curves of bare and graphene/CMOG-coated glassy carbon electrodes (adapted from [68])

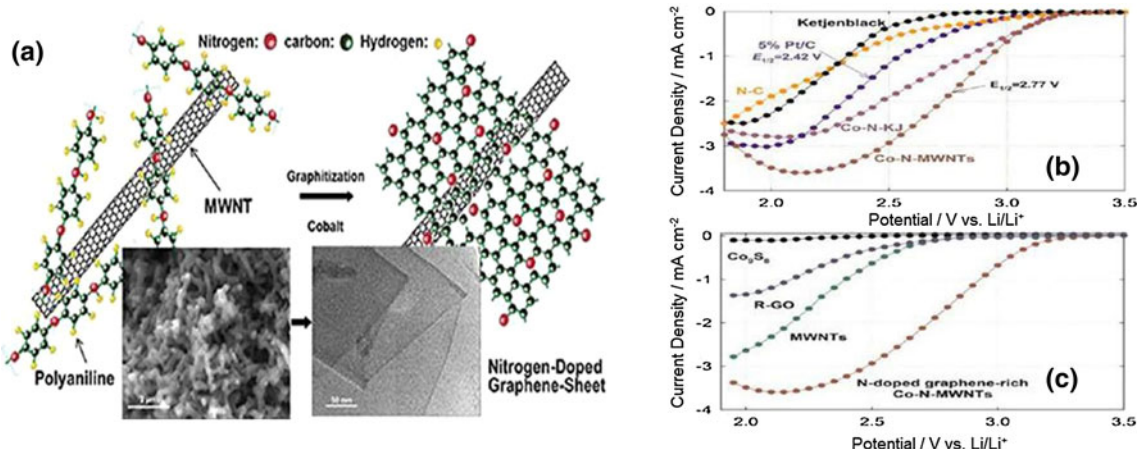

Fig. 11 SEM images and scheme of the formation of nitrogen-doped graphene sheets derived from polyaniline and Co precursors, using MWNTs as a template: **a** RDE testing results for ORR at 25 °C in oxygen saturated 0.1 M $LiPF_6$ in 1,2-dimethoxyethane electrolyte at a rotating speed 900 rpm, **b** various catalyst samples and controls, and **c** different components found in the best performing Co–N–MWNT composite catalysts (adapted from [69])

collection in alkaline cathodes [72, 75]. In contrast, rechargeable Li–air batteries with the mixture of Pd and mesoporous α-MnO_2 electrode have been investigated [76]. This electrode showed high activity to oxidation and reduction of Li to form Li_2O_2 or Li_2O. The ORR activity of various noble materials such as Pd, Pt, Ruthenium (Ru), and Au has been investigated and compared with GC [77]. The Li^+-ORR activity was found to be Pd > Pt > Ru ~ Au > GC on bulk surfaces. Such a trend of Pd/C, Pt/C, Ru/C, Au/C, and VC, the ORR activity of 100 mA g_{carbon}^{-1} can reach a potential of 2.95, 2.86, 2.84, 2.76, and 2.74 V_{Li}, respectively. Thus, palladium- and silver-based catalysts are promising cathode catalyst materials with good balance between cost and performance.

2.3 Electrolyte

The electrolyte is currently the biggest obstacle to progress in Li–air batteries, receiving intense research attention. The first Li–air battery revealed problems such as O_2 solubility in electrolyte, lithium oxide disbanding, instability of the lithium anode in various electrolytes, especially in aqueous electrolyte, and lack of catalyst for rechargeable batteries. It is impractical to use a lithium anode directly in aqueous electrolytes due to the reactivity between lithium and water in the Li–air battery [78]. A solution has been sought using a solid-state battery [25] and incorporating a mixed electrolyte system [79] to avoid the undesirable reactions between the lithium anode and an aqueous electrolyte. Several types of electrolytes have been investigated in search for a rechargeable Li–air battery.

2.3.1 Organic carbonate

Carbonate-based organic electrolytes such as propylene carbonate (PC) have been widely investigated in Li–air batteries, mostly because carbonate mixtures are the dominant electrolyte solvents in Li-ion batteries and PC has a wide liquid temperature range from −50 to 240 °C and low volatility [80]. Various types of electrolytes have been investigated for use in lithium batteries by dissolving $LiPF_6$ in various solvents [16], notably PC, λ-butyrolactone

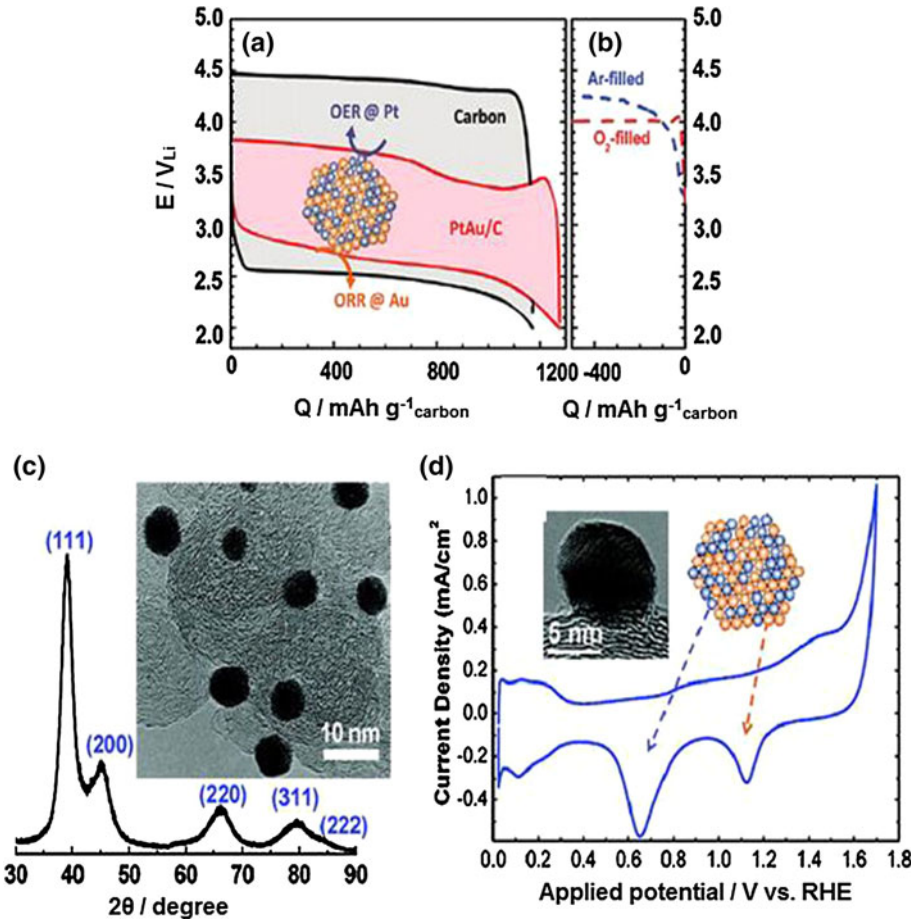

Fig. 12 **a** Lithium–air battery discharge/charge profiles of carbon (*black*, 85 mA g^{-1}_{carbon}) and PtAu/C (*red*, 100 mA g^{-1}_{carbon}) in the third cycle at 0.04 mA cm^{-2} electrode. **b** Background measurement during charging at 100 mA g^{-1}_{carbon} of Ar^{-} and $^{-}O_2$ filled cells for PtAu/C. **c** Representative TEM image and XRD data of PtAu/C. **d** CV of PtAu/C (adapted from [70]). (Color figure online)

(λ-BL), ethylene carbonate (EC), diethyl carbonate (DEC), dimethyl carbonate (DMC), 1,2-dimethoxyethane (DME), tetrahydrofuran (THF), and tetrahydropyran (THP) and their mixtures. It has also been suggested that the viscosity of electrolyte influences the O_2 solubility in the electrolytes: the greater the O_2 solubility the greater the discharge capacity. Lower viscosity ensures higher O_2 solubility of the electrolyte, with a tendency to decomposition. It should be noted that PC:DEC (1:1) solvent exhibited the highest discharge capacity of 2,120 mAh g^{-1}. In addition, O_2 solubility, electrolyte viscosity, and O_2 partial pressure have direct correlation to discharge capacity and rate capability. The O_2 transport properties of several electrolytes have been investigated and the results suggested the dependence of cell performance on O_2 transport in organic electrolyte [81]. It has been reported that specific capacity can be increased from 85 to 500 mAh g^{-1} by increasing O_2 concentration in the electrolyte, either by electrolyte reformulation or by increasing O_2 partial pressure. Furthermore, by decreasing electrolyte viscosity, discharge capacity can be increased [82]. However, it has been reported that such types of electrolytes decompose in Li–air batteries during discharge. Bruce et al. [83] reported that the discharge product in a nonaqueous rechargeable Li–air battery is a mixture of Li and PC (particularly Li_2CO_3), rather than electrochemically reversible Li_2O_2, which severely affects the rechargeability and life cycle of aprotic Li–air batteries.

2.3.2 *Ethers and glymes*

Ethers are also receiving attention for Li–air batteries because they display promising characteristics such as stability with high oxidation potential over 4.5 V vs. Li/Li^+, low volatility such as tetraglyme, the capability to operate with lithium anode, plus being safe and inexpensive [84]. However, ether-based electrolytes, which are being more stable than organic carbonates, still undergo decomposition and producing mixture of Li_2CO_3, HCO_2Li, CO_2, and H_2O [83, 85]. Lu et al. [70] have shown that the polarity of electrolyte is of more concern than the viscosity. Low polarity electrolytes, such as ethers and glymes, can easily wet the surface of a low polarity porous carbon air cathode. Thus, O_2 diffusion through these open channels is much higher than liquid electrolyte because electrolyte floods and infiltrates the porous carbon cathode and reaches a high ORR activity. The flooding of the electrolyte over the porous carbon restricts the O_2 diffusion, and therefore,

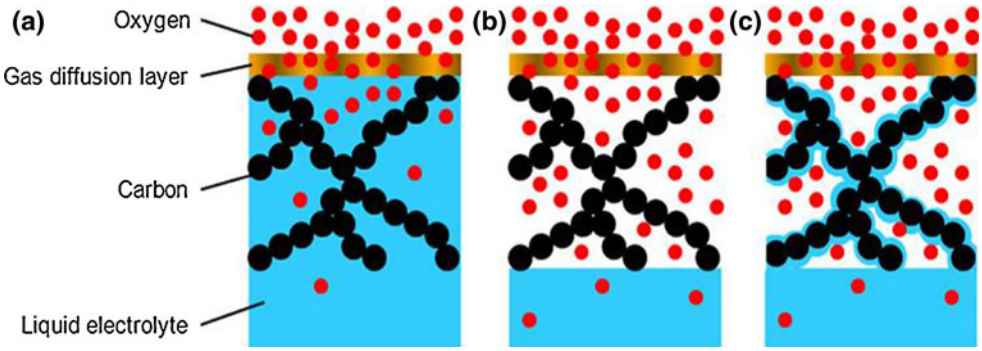

Fig. 13 Schematic view of electrolyte filling in **a** flooded cathode, **b** dry cathode, and **c** wetted cathode (adapted from [87])

it cannot reach a high capacity [86]. In this case, the hybrid electrode combines with a conventional air electrode and the extremely hydrophobic CF_x proposed, which facilitates the airflow channels and allows faster ORR. Based on the electrolyte filling, a Li–air battery cathode can be classified as flooded, dry, or wetted, as shown in Fig. 13 [87]. Firstly, in a flooded cathode, the O_2 has to dissolve into the electrolyte at the cathode–O_2 interface but O_2 is less soluble in a liquid medium than a gaseous medium, and therefore, the kinetics of the system is slow. In contrast, a dry cathode is insufficiently filled with electrolyte and the O_2 can penetrate easier and deeper into the cathode but lithium ion will only be present at the cathode–electrolyte interface. Therefore, more reaction products will form at the cathode–electrolyte interface. However, a wetted cathode is free from the problems associated with a dry or a flooded cathode except the slow air diffusion [87].

2.3.3 Solid-state electrolytes

Current thin-film solid-state Li–air batteries based on lithium phosphorous oxynitride (LIPON) electrolytes have been shown to have reasonable life cycles (more than 1,000 times) but, unfortunately, LIPON has low ionic conductivity (10^{-6} S cm^{-1} at 25 °C) [88]. Low ionic conductivity, particularly at low temperatures, means that electrolytes need a very thick lithium electrode. It should be noted that a thick electrode is more suitable for an aqueous rather than a nonaqueous Li–air cell because of the higher conductivity of aqueous electrolyte solutions. However, a thick electrode is necessary in order to achieve high energy density, although thick electrode implies a poor power density [89].

2.3.4 Ionic liquids

Taking into consideration the limitation of solid-state-type electrolytes, a high ionic conductive, extremely low electronic conductive, and chemically or electrochemically stable solid-state electrolyte lithium superionic conductor (LiSICON) have been proposed [90, 91]. This has been demonstrated to be the highest ionic conductivity among any solid-state ionic conductive electrolytes (>10^{-3} S cm^{-1} at 25 °C). In contrast, room temperature ionic liquids (e.g., 1-alkyl-3-methylimidazolium [64]) have attracted much attention due to their special properties such as low flammability, their hydrophobic nature, low vapor pressure, their wide potential window, and high thermal stability [64, 92]. It exhibited a discharge capacity >5,000 mAh g^{-1} of carbon at the very low discharge current of 0.01 mA cm^{-2} with hydrophobicity and negligible vapor pressure. Therefore, ionic liquid Hg/1-ethyl-3-methyl imidazolium imide is considered to be a promising candidate as an electrolyte for a Li–air battery [93]. However, the pyrrolidium-based ionic liquids were found to be more stable than the imidazolium-based ionic liquids, although lower discharge capacities were found in the pyrrolidium-based ionic liquid electrolytes. In addition, the chemical reaction of lithium metal with an aqueous electrolyte and moisturizing nonaqueous electrolyte from air is a great concern. Dual electrolyte lithium air cells, employing NASICON-type solid electrolytes ($Li_{1+x+y}Al_xTi_{2-x}SiyP_{3-y}O_{12}$ or LTAP), have been presented: a lithium metal electrode in nonaqueous electrolyte and O_2 electrode operates in an aqueous electrolyte [94]. This cell exhibited a typical three-stage discharge capacity of 740 mAh g^{-1} that was 90.2 % of the theoretical capacity of buffer solution containing H_3PO_4 (820 mAh g^{-1}), and cell voltage on average 3.3 V with energy density of 2,442 Wh kg^{-1}. Recently, Peng et al. [95] reported a design that employed dimethyl sulfoxide as the electrolyte and gold nanoparticles as the cathode, with 100 charge cycles and only a 5 % capacity loss. This research highlights the importance of developing a stable electrolyte in order to achieve high-performance Li–air battery.

To date, various types of electrolytes have been studied but their electrochemical performance, viscosity, ion conductance tendency, and discharge mechanisms are still not well understood, necessitating further research in this area. Table 2 lists the electrolytes used in Li–air battery covered in this review.

Table 2 Summary of electrolytes used in lithium–air batteries

Types	Examples	Properties	References
Organic carbonate	$LiPF_6$ is dissolved in propylene carbonate (PC), λ-butyrolactone (λ-BL), ethylene carbonate (EC), diethyl carbonate (DEC), dimethyl carbonate (DMC), 1,2-dimethoxyethane (DME), tetrahydrofuran (THF), and tetrahydropyran (THP)	Low viscous which ensure high oxygen solubility Low volatility Compatible with lithium metal High discharge capacity and electrolytes can decompose	[16, 83]
Ethers and glymes	$LiPF_6$ in tetraethylene glycol dimethyl ether, and tetraglyme	Low volatility High stable with lithium anode. High oxidation potential of 4.5 V More stable than carbonate base electrolytes Low polarity Easily wet the low polarity carbon cathode	[84–86]
Ionic liquids	1-Alkyl-3-methylimidazolium, Hg/1-ethyl-3-methyl imidazolium imide	Low flammability, hydrophobic nature, low vapor pressure, wide potential window, and high thermal stability. High viscous and low ionic conductivity	[64, 92, 93]
Solid-state electrolytes	Lithium phosphorous oxynitride (LIPON), lithium superionic conductor (LiSICON), NASICON (LTAP), glass–ceramic, and polymer ceramic	Thermal stability, Chemical stability and rechargeability Act as a separator Low ionic conductivity, particularly at low temperatures	[25, 26, 88, 90, 91, 94]

2.4 Lithium metal anode

Lithium metal is the anode of choice for lithium–air cells because of their high energy density compared to lithium intercalation anodes. They have the most electropositivity, −3.04 V versus a standard hydrogen electrode (SHE), and are the lightest metal (standard atomic weight 6.941 g mol^{-1} and specific gravity = 0.53 g cm^{-1}) with the highest specific capacity 3,860 Ah kg^{-1}. The implementation of lithium metal anodes, however, is believed to be problematic. Lithium metal and liquid electrolytes react violently and degrade the lithium metal in the formation of a mosaic structure of lithium metal surface. Thus, a solid electrolyte interphase (SEI) layer is formed as a multilayer structure. This chemical heterogeneity of the SEI results in a morphologically heterogeneous structure, leading to nonuniform current distribution. This inhomogeneous current distribution causes further dendrite growth and typically leads to a short-circuit between the anode and cathode. In contrast, in an aqueous electrolyte, this SEI is placed artificially to reduce the reactivity of lithium metal with water [96]. Failure mechanisms of Li metal anodes at high charging rates have been investigated [97]. It was shown that at high charging rates, lithium deposition produces small grains, which are highly reactive with the electrolyte solution. Li metal anode fails due to the extremely high discharge–charge current densities developed as the active electrode area decreases. These high currents lead to the formation of dendrites that short-circuit the battery, thus terminating its life [97]. The characteristics of Li/MnO_2 cells using compacted Li powder and Li foil as anode have been investigated at high-rate discharge [98]. Cells using compacted Li powder anodes show larger capacity (216 mAh compared with a Li foil cell of 164 mAh at 0.2 mA standard current) and lower internal resistance (ranging from 13 to 100 Ω compared with a Li foil cell of 17–250 Ω) than cells using Li metal foil anodes. Recently, a similar kind of investigation has been done by Kong et al. [99] for the prevention of Li dendrite growth in Li metal secondary cells. It has been reported that porous Li powder electrodes, which is formed by using droplet emulsion, were free from observable growth of dendrites formation after 250 charge–discharge (C–D) cycles, whereas dendrite growth was observed on the surface of the Li foil electrode only after 10 C–D cycles. It is, therefore, a matter of fact that dendrite formation or a degrading lithium metal electrode in aqueous electrolyte needs to overcome to enable better performance of the Li–air battery. To protect the lithium anode, an artificial SEI is needed to cover it. A substantial amount of potential energy is necessary during the lithium ions transfer through the SEI layer to the electrolytes. Generally, SEI consists of two layers: (1) inorganic compounds such as Li and Li_2CO_3, which are basically formed by lithium metal

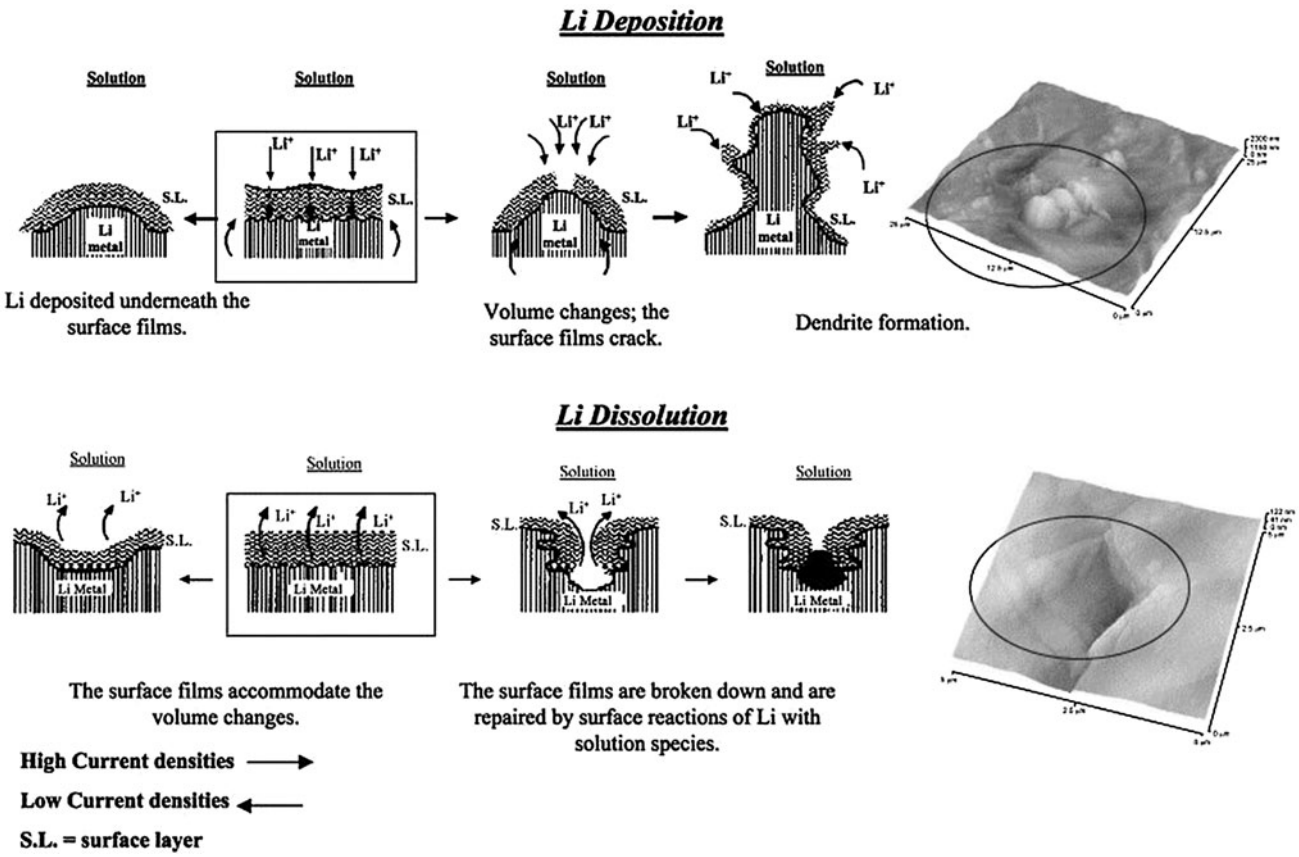

Fig. 14 Morphology and failure mechanism of solid electrolyte interphase (SEI) (adapted from [101])

reacting with atmospheric O_2, H_2O, CO_2 or N_2, and (2) an organic compound of HC, electrolytes, and lithium metal [100]. This complex compound is formed on the SEI layer until the battery is completely discharged. It shows unexpected electrochemical behaviors such as low cycling efficiency, gradual capacity loss, and poor cyclability [100]. The SEI layer can be easily cracked and broken during lithium metal deposition and dissolution. The deposition of lithium metal could not be fully completed due to contact with the electrolytes that finally degrades the lithium metal anode and form a heterogeneous layer. This heterogeneous layer leads to nonuniform current density. The local current density at the edge of the lithium anode is the main reason for the heterogeneous layer/dendrite formation of lithium metal. This creates exothermic conditions and can burst and ignites the battery. Figure 14 is a description of the morphology and failure mechanism of lithium electrodes during lithium metal deposition and dissolution [101].

Numerous attempts have been made to remedy the process and to improve rechargeability. Some of them are given below:

a. Choosing an electrolyte of liquid or polymer that is less reactive with lithium metal [102].
b. Forming a SEI layer by adding CO_2, HF, or S_x^{2-} to the electrolytes so that it can react with the lithium surface to form a SEI layer. This then acts as a SEI inner layer to subdue dendrite formation. The addition of a small amount of HF in the electrolytes forms LiF on the lithium surface and gives a smooth surface.
c. Using hydrocarbon or quaternary ammonium salt as an active agent on the surface of the lithium metal [103].
d. Placing an ultra-thin plasma polymer layer on the surface of the lithium metal. The lithium metal surface is covered by a solid polymer that is prepared via plasma polymerization of 1, 1-difluoroethene ($C_2H_4F_2$) and inhibits dendrite formation [104]. In addition, polyethylene glycol dimethacrylate is solid and thin, allowing the electrons to pass to the electrolytes and cover the surface of the anode, keeping it smooth [105].
e. Formation of a stable metal alloy (LiI) by incorporating tin(II) iodide (SnI_2) or aluminum iodide AlI_3, SnI_2, and AlI_3 have been investigated and found as promising additives for improving cyclic efficiency for the lithium electrode [106]. It is postulated that the thin layers of the lithium alloys at the lithium electrode surface result in an improvement of Coulombic

efficiency (especially after 10th cycle) during lithium deposition and dissolution.

f. Formation of an ultra-thin polymer electrolyte layer based on ultraviolet (UV) irradiation polymerization or plasma polymerization [107, 108]. The formation of semi-interpenetrating network (semi-IPN) structure protective layer on lithium electrodes was attempted to make the lithium deposition morphology less dendritic. The UV-curable mixed solution consists of linear polymer (Kynar 2801), crosslinking agent (1,6-hexanediol diacrylate), liquid electrolyte (EC/PC/1 M $LiClO_4$), oligo(ethylene glycol) borate (OEGB) anion receptor, and photoinitiator (methyl benzoylformate). This curable mixed solution was directly coated on the lithium metal surface, and it was UV-irradiated by UV light for 2 min after drying. Eventually, a protective layer based on semi-IPN structure was formed on the lithium metal surface [107].

g. Uniform lithium deposition by means of pressure and temperature [109–111]. In situ investigation of dendritic lithium growth during cycling has been carried out [111]. Mechanical pressure has shown to have a crucial effect on lithium morphology, lithium cyclability, and dendritic lithium growth. This is because lithium was deposited densely and uniformly on the lithium electrode surfaces under pressure, and the isolation of deposited lithium from the electrode during the lithium stripping process was reduced. In addition, low temperature conditions (from −10 to 0 °C) could improve the C–D cycling efficiency of lithium metal of nickel substrate [110].

3 Summary

There has been exciting progresses in the area of Li–air batteries over the past decade. Nevertheless, there are still many challenges facing the design of rechargeable Li–air batteries such as cathode degradation by environmental humidity, blockage of the porous carbon cathode, decomposition of the electrolyte during charge and discharge, and the highly reactive Li anode with atmospheric moisture. In this review, the fundamentals and recent progresses in the field of Li–air batteries have been insightfully summarized. The following main points have been addressed:

1. A cathode reaction delivers most of the energy because most of the cell voltage drop occurs at the air cathode. It is thought that nonaqueous Li–air energy falls far too short of the theoretical values because the discharge terminates well before all the pores in the air electrode (porous carbon) are filled with lithium oxide or peroxides. Therefore, it is essential to optimize the porous structure of a carbon electrode.
2. The catalyst has a significant effect on the cathode reaction. Several catalysts have been proposed for charging and discharging and some are still in progress. MnO_2 and PtAu nanoparticles have shown good stability against OER and ORR. However, the cost of Au- and Pt-based catalysts is still prohibitive for commercialization. Therefore, more efforts should be given to the development of a cost-effective Li–air battery.
3. Currently, most aprotic Li–air batteries operate with pure O_2. Environmental O_2 is combined with moisture, which could degrade the nonaqueous electrolyte and lithium metal anode, and therefore, the battery has a poor life cycle compared with current lithium–ion batteries. O_2 separation from air for the Li–air is a problem as teflonized layer membrane can only slow down H_2O ingress. Therefore, intensive investigation is necessary to better understand the O_2 solubility and diffusivity in electrolytes (both aqueous and nonaqueous), and the viscosity and polarity factors of the electrolytes.
4. The development of novel electrolytes with the properties of low viscous, low volatility, compatible with electrodes, hydrophobic, high O_2 solubility or diffusivity, thermal and chemically stable, and less decomposing electrolytes, which will not release CO_2 during charging, is the biggest challenges. Therefore, modifications of existing electrolytes and the quest for new electrolyte systems present new challenges for progress in the lithium–air battery.
5. The main problem associated with lithium metal as the anode is dendrite formation. This dendrite formation is heterogeneous, which can lead to dangerous battery short-circuiting and poor cycle performance. However, this can be suppressed by the formation of a stable SEI film on the surface of the lithium anode. Therefore, in order to combat this problem, a novel solid polymer electrolyte has been introduced to protect the lithium metal and conducts lithium ions, thereby preventing dendrite formation.

Acknowledgments The authors acknowledge financial support for this research through the Australia–India Strategic Research Fund (AISRF, ST 060048).

References

1. Soloveichik GL (2011) Battery technologies for large-scale stationary energy storage. Annu Rev Chem Biomol Eng 2:503–527. doi:10.1146/annurev-chembioeng-061010-114116

2. Winter M, Brodd RJ (2004) What are batteries, fuel cells, and supercapacitors? Chem Rev 104:4245–4269
3. Tarascon J-M, Armand M (2001) Issues and challenges facing rechargeable lithium batteries. Nature 414(6861):359–367
4. Armand M, Tarascon JM (2008) Building better batteries. Nature 451(7179):652–657
5. Anderman M, Kalhammer FR, MacArthur D (2000) Advanced batteries for electric vehicles: an assessment of performance, cost, and availability. Prepared for State of California Air Resources Board, Sacramento
6. Taniguchi A, Fujioka N, Ikoma M, Ohta A et al (2001) Development of nickel/metal-hydride batteries for EVs and HEVs. J Power Sources 100(1–2):117–124. doi:10.1016/S0378-7753(01)00889-8
7. Scrosati B, Garche J (2010) Lithium batteries: status, prospects and future. J Power Sources 195(9):2419–2430
8. Girishkumar G, McCloskey B, Luntz AC, Swanson S, Wilcke W (2010) Lithium-air battery: promise and challenges. J Phys Chem Lett 1(14):2193–2203
9. Zheng J, Liang R, Hendrickson M, Plichta E (2008) Theoretical energy density of Li–air batteries. J Electrochem Soc 155(6): A432–A437
10. Kraytsberg A, Ein-Eli Y (2011) Review on Li–air batteries—opportunities, limitations and perspective. J Power Sources 196(3):886–893
11. Lu YC, Gasteiger HA, Parent MC, Chiloyan V, Shao-Horn Y (2010) The influence of catalysts on discharge and charge voltages of rechargeable Li–oxygen batteries. Electrochem Solid-State Lett 13(6):A69–A72
12. Zhang T, Imanishi N, Shimonishi Y, Hirano A, Takeda Y, Yamamoto O, Sammes N (2010) A novel high energy density rechargeable lithium/air battery. Chem Commun 46(10): 1661–1663
13. Xu W, Xu K, Viswanathan VV, Towne SA, Hardy JS, Xiao J, Nie Z, Hu D, Wang D, Zhang J-G (2011) Reaction mechanisms for the limited reversibility of Li–O_2 chemistry in organic carbonate electrolytes. J Power Sources 196(22):9631–9639. doi:10.1016/j.jpowsour.2011.06.099
14. Hardwick LJ, Bruce PG (2012) The pursuit of rechargeable non-aqueous lithium–oxygen battery cathodes. Curr Opin Solid State Mater Sci 16:178–185
15. Abraham K, Jiang Z (1996) A polymer electrolyte-based rechargeable lithium/oxygen battery. J Electrochem Soc 143(1): 1–5
16. Read J (2002) Characterization of the lithium/oxygen organic electrolyte battery. J Electrochem Soc 149(9):A1190–A1195
17. Ogasawara T, Débart A, Holzapfel M, Novák P, Bruce PG (2006) Rechargeable Li_2O_2 electrode for lithium batteries. J Am Chem Soc 128(4):1390–1393. doi:10.1021/ja056811q
18. Peng Z, Freunberger SA, Hardwick LJ, Chen Y, Giordani V, Bardé F, Novák P, Graham D, Tarascon JM, Bruce PG (2011) Oxygen reactions in a non-aqueous Li^+ electrolyte. Angew Chem Int Ed 123(28):6475–6479
19. Cheng H, Scott K (2011) Selection of oxygen reduction catalysts for rechargeable lithium–air batteries—metal or oxide? Appl Catal B 108:140–151
20. Laoire CO, Mukerjee S, Abraham K, Plichta EJ, Hendrickson MA (2010) Influence of nonaqueous solvents on the electrochemistry of oxygen in the rechargeable lithium− air battery. J Phys Chem C 114(19):9178–9186
21. Zhong L, Mitchell RR, Liu Y, Gallant BM, Thompson CV, Huang JY, Mao SX, Shao-Horn Y (2013) In situ transmission electron microscopy observations of electrochemical oxidation of Li_2O_2. Nano Lett 13(5):2209–2214
22. Xu K (2004) Nonaqueous liquid electrolytes for lithium-based rechargeable batteries. Chem Rev Columb 104(10):4303–4418
23. Kowalczk I, Read J, Salomon M (2007) Li-air batteries: a classic example of limitations owing to solubilities. Pure Appl Chem 79(5):851–860
24. He P, Wang Y, Zhou H (2010) A Li-air fuel cell with recycle aqueous electrolyte for improved stability. Electrochem Commun 12(12):1686–1689
25. Kumar B, Kumar J, Leese R, Fellner JP, Rodrigues SJ, Abraham KM (2010) A solid-state, rechargeable, long cycle life lithium-air battery. J Electrochem Soc 157(1):50–54
26. Kumar B, Kumar J (2010) Cathodes for solid-state lithium–oxygen cells: roles of NASICON glass-ceramics. J Electrochem Soc 157(5):A611–A616
27. Zhang LL, Wang ZL, Xu D, Zhang XB, Wang LM (2012) The development and challenges of rechargeable non-aqueous lithium–air batteries. Int Smart Nano Mater 1:1–20
28. Yoo E, Zhou H (2011) Li-air rechargeable battery based on metal-free graphene nanosheet catalysts. ACS Nano 5(4):3020–3026
29. Zhang SS, Foster D, Read J (2010) Discharge characteristic of a non-aqueous electrolyte Li/O_2 battery. J Power Sources 195(4): 1235–1240
30. Whittingham MS (2012) Metal-air batteries: a reality check. Electrochem Soc, PRiME, Honolulu, USA
31. Xiao J, Wang D, Xu W, Williford RE, Liu J, Zhang JG (2010) Optimization of air electrode for Li/air batteries. J Electrochem Soc 157(4):A487–A492
32. Yang Y, Sun Q, Li YS, Li H, Fu ZW (2011) Nanostructured diamond like carbon thin film electrodes for lithium air batteries. J Electrochem Soc 158(10):B1211–B1216
33. Wang Y, Cheng L, Li F, Xiong H, Xia Y (2007) High electrocatalytic performance of Mn_3O_4/mesoporous carbon composite for oxygen reduction in alkaline solutions. Chem Mater 19(8):2095–2101
34. Williford RE, Zhang JG (2009) Air electrode design for sustained high power operation of Li/air batteries. J Power Sources 194(2):1164–1170
35. Stevens P, Toussaint G, Vinatier P, Puech L (2012) Very high specific surface area capacity lithium-air battery. Electrochem Soc, PRiME, Honolulu, USA
36. Cheng H, Scott K (2010) Carbon-supported manganese oxide nanocatalysts for rechargeable lithium–air batteries. J Power Sources 195(5):1370–1374. doi:10.1016/j.jpowsour.2009.09.030
37. Yang XH, He P, Xia Y-y (2009) Preparation of mesocellular carbon foam and its application for lithium/oxygen battery. Electrochem Commun 11(6):1127–1130. doi:10.1016/j.elecom.2009.03.029
38. Mirzaeian M, Hall PJ (2009) Preparation of controlled porosity carbon aerogels for energy storage in rechargeable lithium oxygen batteries. Electrochim Acta 54(28):7444–7451
39. Ren X, Zhang SS, Tran DT, Read J (2011) Oxygen reduction reaction catalyst on lithium/air battery discharge performance. J Mater Chem 21(27):10118–10125
40. Arai H, Müller S, Haas O (2000) AC impedance analysis of bifunctional air electrodes for metal-air batteries. J Electrochem Soc 147(10):3584–3591
41. Ottakam Thotiyl MM, Freunberger SA, Peng Z, Bruce PG (2013) The carbon electrode in nonaqueous Li–O_2 cells. J Am Chem Soc 135(1):494–500
42. Ohkuma H, Uechi I, Matsui M, Takeda Y, Yamamoto O, Imanishi N (2014) Stability of carbon electrodes for aqueous lithium-air secondary batteries. J Power Sources 245:947–952
43. Song MK, Park S, Alamgir FM, Cho J, Liu M (2011) Nanostructured electrodes for lithium-ion and lithium-air batteries: the latest developments, challenges, and perspectives. Mater Sci Eng R 72(11):203–252
44. Mitchell RR, Gallant BM, Thompson CV, Shao-Horn Y (2011) All-carbon-nanofiber electrodes for high-energy rechargeable Li–O_2 batteries. Energy Environ Sci 4(8):2952–2958

45. Jiang K, Wang J, Li Q, Liu L, Liu C, Fan S (2011) Superaligned carbon nanotube arrays, films, and yarns: a road to applications. Adv Mater 23(9):1154–1161
46. Gong KP, Du F, Xia ZH, Durstock M, Dai LM (2009) Nitrogen-doped carbon nanotube arrays with high electrocatalytic activity for oxygen reduction. Science 323(5915):760–764
47. Tang Y, Allen BL, Kauffman DR, Star A (2009) Electrocatalytic activity of nitrogen-doped carbon nanotube cups. J Am Chem Soc 131(37):13200–13201
48. Li H, Liu H, Jong Z, Qu W, Geng D, Sun X, Wang H (2011) Nitrogen-doped carbon nanotubes with high activity for oxygen reduction in alkaline media. Int J Hydrogen Energy 36(3): 2258–2265
49. Shao Y, Wang X, Engelhard M, Wang C, Dai S, Liu J, Yang Z, Lin Y (2010) Nitrogen-doped mesoporous carbon for energy storage in vanadium redox flow batteries. J Power Sources 195(13):4375–4379. doi:10.1016/j.jpowsour.2010.01.015
50. Kichambare P, Kumar J, Rodrigues S, Kumar B (2011) Electrochemical performance of highly mesoporous nitrogen doped carbon cathode in lithium–oxygen batteries. J Power Sources 196(6):3310–3316
51. Kichambare P, Rodrigues S, Kumar J (2012) Mesoporous nitrogen-doped carbon-glass ceramic cathodes for solid-state lithium–oxygen batteries. ACS Appl Mater Interfaces 4:49–52
52. Li Y, Wang J, Li X, Liu J, Geng D, Yang J, Li R, Sun X (2011) Nitrogen-doped carbon nanotubes as cathode for lithium–air batteries. Electrochem Commun 13(7):668–672
53. Xiao J, Mei D, Li X, Xu W, Wang D, Graff GL, Bennett WD, Nie Z, Saraf LV, Aksay IA (2011) Hierarchically porous graphene as a lithium–air battery electrode. Nano Lett 11(11): 5071–5078
54. Li Y, Wang J, Li X, Geng D, Li R, Sun X (2011) Superior energy capacity of graphene nanosheets for a nonaqueous lithium-oxygen battery. Chem Commun 47(33):9438–9440
55. Sun B, Wang B, Su D, Xiao L, Ahn H, Wang G (2012) Graphene nanosheets as cathode catalysts for lithium-air batteries with an enhanced electrochemical performance. Carbon 50(2):727–733
56. Li Y, Wang J, Li X, Geng D, Banis MN, Li R, Sun X (2012) Nitrogen-doped graphene nanosheets as cathode materials with excellent electrocatalytic activity for high capacity lithium-oxygen batteries. Electrochem Commun 18:12–15. doi:10.1016/j.elecom.2012.01.023
57. Li Y, Wang J, Li X, Geng D, Banis MN, Tang Y, Wang D, Li R, Sham TK, Sun X (2012) Discharge product morphology and increased charge performance of lithium-oxygen batteries with graphene nanosheet electrodes: the effect of sulphur doping. J Mater Chem 22:20170–20174
58. Adams BD, Oh SH, Black Robert, Baran-Harper A, Nazar LF (2012) Investigation of ORR and OER in non-aqueous (and aqueous) Li-O_2 cells using metal oxide catalysts. Electrochem Soc, PRiME, Honolulu, USA
59. Dobley A, DiCarlo J, Abraham K et al (2004) Non-aqueous lithium-air batteries with an advanced cathode structure. In: Yardley Technical Products, Inc./Lithion, Inc. Pawcatuck, CT 41st Power Sources Conference Proceedings, Philadelphia, PA
60. Zhang G, Zheng J, Liang R, Zhang C, Wang B, Au M, Hendrickson M, Plichta E (2011) α-MnO2/carbon nanotube/carbon nanofiber composite catalytic air electrodes for rechargeable lithium-air batteries. J Electrochem Soc 158(7):A822–A827
61. Débart A, Bao J, Armstrong G, Bruce PG (2007) An O_2 cathode for rechargeable lithium batteries: the effect of a catalyst. J Power Sources 174(2):1177–1182
62. Débart A, Paterson AJ, Bao J, Bruce PG (2008) α-MnO_2 nanowires: a catalyst for the O_2 electrode in rechargeable lithium batteries. Angew Chem Int Ed 120(24):4597–4600
63. Orellana W (2012) Metal-phthalocyanine functionalized carbon nanotubes as catalyst for the oxygen reduction reaction: a theoretical study. Chem Phys Lett 541:81–84
64. Kuboki T, Okuyama T, Ohsaki T, Takami N (2005) Lithium-air batteries using hydrophobic room temperature ionic liquid electrolyte. J Power Sources 146(1–2):766–769. doi:10.1016/j.jpowsour.2005.03.082
65. Zhang SS, Ren X, Read J (2011) Heat-treated metal phthalocyanine complex as an oxygen reduction catalyst for non-aqueous electrolyte Li/air batteries. Electrochim Acta 56(12): 4544–4548. doi:10.1016/j.electacta.2011.02.072
66. Kim H, Lee K, Woo SI, Jung Y (2011) On the mechanism of enhanced oxygen reduction reaction in nitrogen-doped graphene nanoribbons. Phys Chem Chem Phys 13(39):17505–17510
67. Lee DU, Yu A, Park HW, Nickel CZ (2012) Cobalt oxide nanostructures on graphene as an active bifunctional electrocatalyst. Electrochem Soc, PRiME, Honolulu, USA
68. Wang L, Zhao X, Lu Y, Xu M, Zhang D, Ruoff RS, Stevenson KJ, Goodenough JB (2011) $CoMn_2O_4$ spinel nanoparticles grown on graphene as bifunctional catalyst for lithium-air batteries. J Electrochem Soc 158(12):A1379–A1382
69. Wu G, Mack NH, Gao W, Ma S, Zhong R, Han J, Baldwin JK, Zelenay P (2012) Nitrogen-doped graphene-rich catalysts derived from heteroatom polymers for oxygen reduction in nonaqueous lithium–O_2 battery cathodes. ACS Nano 6(11): 9764–9776
70. Lu YC, Xu Z, Gasteiger HA, Chen S, Hamad-Schifferli K, Shao-Horn Y (2010) Platinum− gold nanoparticles: a highly active bifunctional electrocatalyst for rechargeable lithium− air batteries. J Am Chem Soc 132(35):12170–12171
71. Bian X, Guo K, Liao L, Xiao J, Kong J, Ji C, Liu B (2012) Nanocomposites of palladium nanoparticle-loaded mesoporous carbon nanospheres for the electrochemical determination of hydrogen peroxide. Talanta 99:256–261
72. Bidault F, Kucernak A (2011) Cathode development for alkaline fuel cells based on a porous silver membrane. J Power Sources 196(11):4950–4956
73. Erikson H, Sarapuu A, Alexeyeva N, Tammeveski K, Solla-Gullón J, Feliu J (2012) Electrochemical reduction of oxygen on palladium nanocubes in acid and alkaline solutions. Electrochim Acta 59:329–335
74. Spendelow JS, Wieckowski A (2007) Electrocatalysis of oxygen reduction and small alcohol oxidation in alkaline media. Phys Chem Chem Phys 9(21):2654–2675
75. Tang W, Zhang L, Henkelman G (2011) Catalytic activity of Pd/Cu random alloy nanoparticles for oxygen reduction. J Phys Chem Lett 2(11):1328–1331
76. Thapa AK, Ishihara T (2011) Mesoporous α-MnO_2/Pd catalyst air electrode for rechargeable lithium–air battery. J Power Sources 196(16):7016–7020. doi:10.1016/j.jpowsour.2010.09.112
77. Lu Y-C, Gasteiger HA, Shao-Horn Y (2011) Catalytic activity trends of oxygen reduction reaction for nonaqueous Li-air batteries. J Am Chem Soc 133(47):19048–19051
78. Zhang T, Imanishi N, Shimonishi Y, Hirano A, Xie J, Takeda Y, Yamamoto O, Sammes N (2010) Stability of a water-stable lithium metal anode for a lithium–air battery with acetic acid–water solutions. J Electrochem Soc 157(2):A214–A218
79. Wang Y, He P, Zhou H (2011) A lithium–air capacitor–battery based on a hybrid electrolyte. Energy Environ Sci 4(12):4994–4999
80. Shao Y, Ding F, Xiao J, Zhang J, Xu W, Park S, Zhang JG, Wang Y, Liu J (2012) Making Li/air batteries rechargeable: material challenges. Adv Funct Mater 23(8):987–1004
81. Read J, Mutolo K, Ervin M, Behl W, Wolfenstine J, Driedger A, Foster D (2003) Oxygen transport properties of organic

electrolytes and performance of lithium/oxygen battery. J Electrochem Soc 150(10):A1351–A1356
82. Wu B, Chen X, Zhang C, Mu D, Wu F (2012) Lithium–air and lithium–copper batteries based on a polymer stabilized interface between two immiscible electrolytic solutions (ITIES). New J Chem 36(10):2140–2145
83. Freunberger SA, Chen Y, Peng Z, Griffin JM, Hardwick LJ, Bardé F, Novák P, Bruce PG (2011) Reactions in the rechargeable lithium–O_2 battery with alkyl carbonate electrolytes. J Am Chem Soc 133(20):8040–8047. doi:10.1021/ja2021747
84. CormacÓ Laoire SM, Plichta EJ, Hendrickson MA, Abraham KM (2011) Rechargeable lithium/TEGDME- $LiPF_6/O_2$ battery batteries and energy storage. J Electrochem Soc 158(3):A302–A308
85. Freunberger SA, Chen Y, Drewett NE, Hardwick LJ, Bardé F, Bruce PG (2011) The lithium–oxygen battery with ether-based electrolytes. Angew Chem Int Ed 50(37):8609–8613. doi:10.1002/anie.201102357
86. Xu W, Xiao J, Wang D, Zhang J, Zhang JG (2010) Effects of nonaqueous electrolytes on the performance of lithium/air batteries. J Electrochem Soc 157(2):A219–A224
87. Padbury R, Zhang X (2011) Lithium–oxygen batteries—limiting factors that affect performance. J Power Sources 196(10):4436–4444
88. Yu X, Bates J, Jellison G, Hart F (1997) A stable thin-film lithium electrolyte: lithium phosphorus oxynitride. J Electrochem Soc 144(2):524–532
89. Christensen J, Albertus P, Sanchez-Carrera RS, Lohmann T, Kozinsky B, Liedtke R, Ahmed J, Kojic A (2011) A critical review of Li/air batteries. J Electrochem Soc 159(2):R1–R30
90. Christopher P, Rhodes YF, Mullings M, Uselton K, Cross J Solid-state lithium batteries using thio-LISICON solid-state electrolytes. Lynntech, Inc. 7610 Eastmark Dr., College Station, TX 77840. https://web.ornl.gov/ccsd_registrations/battery/abstracts/Solidstate%20batteries_abstract_Rhodes_2010-08-30.pdf. Accessed 25 April 2013
91. Thangadurai V (2012) Recent developments in solid Li-ion electrolytes. PRiME, Honolulu
92. Zhang D, Li R, Huang T, Yu A (2010) Novel composite polymer electrolyte for lithium air batteries. J Power Sources 195(4):1202–1206
93. Nanjundiah C, McDevitt S, Koch V (1997) Differential capacitance measurements in solvent-free ionic liquids at Hg and C interfaces. J Electrochem Soc 144(10):3392–3397
94. Manthiram A, Li L, Fu Y (2012) Dual-electrolyte lithium-air batteries with buffer catholytes. Electrochem Soc, PRiME, Honolulu, USA
95. Peng Z, Freunberger SA, Chen Y, Bruce PG (2012) A reversible and higher-rate Li-O_2 battery. Science 337(6094):563–566
96. Whittingham MS (1976) Electrical energy storage and intercalation chemistry. Science 192(4244):1126–1127
97. Aurbach D, Zinigrad E, Teller H, Dan P (2000) Factors which limit the cycle life of rechargeable lithium (metal) batteries. J Electrochem Soc 147(4):1274–1279
98. Park MS, Yoon WY (2003) Characteristics of a Li/MnO_2 battery using a lithium powder anode at high-rate discharge. J Power Sources 114(2):237–243. doi:10.1016/S0378-7753(02)00581-5
99. Kong S-K, Kim B-K, Yoon W-Y (2012) Electrochemical behavior of Li-powder anode in high Li capacity used. J Electrochem Soc 159(9):A1551–A1553
100. Aurbach D, Talyosef Y, Markovsky B, Markevich E, Zinigrad E, Asraf L, Gnanaraj JS, Kim H-J (2004) Design of electrolyte solutions for Li and Li-ion batteries: a review. Electrochim Acta 50(2–3):247–254. doi:10.1016/j.electacta.2004.01.090
101. Aurbach D, Zinigrad E, Cohen Y, Teller H (2002) A short review of failure mechanisms of lithium metal and lithiated graphite anodes in liquid electrolyte solutions. Solid State Ion 148(3–4):405–416. doi:10.1016/S0167-2738(02)00080-2
102. Novák P, Müller K, Santhanam K, Haas O (1997) Electrochemically active polymers for rechargeable batteries. Chem Rev 97(1):207–282
103. Pokhodenko VD, Koshechko VG, Krylov VA (1993) New electrolytes and polymer cathode materials for lithium batteries. J Power Sources 45(1):1–5. doi:10.1016/0378-7753(93)80001-6
104. Takehara Z-i, Ogumi Z, Uchimoto Y, Yasuda K, Yoshida H (1993) Modification of lithium/electrolyte interface by plasma polymerization of 1,1-difluoroethene. J Power Sources 44(1–3):377–383. doi:10.1016/0378-7753(93)80177-Q
105. Lee YM, Choi NS, Park JH, Park JK (2003) Electrochemical performance of lithium/sulfur batteries with protected Li anodes. J Power Sources 119:964–972
106. Matsuda Y, Ishikawa M, Yoshitake S, Morita M (1995) Characterization of the lithium-organic electrolyte interface containing inorganic and organic additives by in situ techniques. J Power Sources 54(2):301–305
107. Choi N-S, Lee YM, Cho KY, Ko D-H, Park J-K (2004) Protective layer with oligo (ethylene glycol) borate anion receptor for lithium metal electrode stabilization. Electrochem Commun 6(12):1238–1242. doi:10.1016/j.elecom.2004.09.023
108. Choi N-S, Lee YM, Seol W, Lee JA, Park J-K (2004) Protective coating of lithium metal electrode for interfacial enhancement with gel polymer electrolyte. Solid State Ion 172(1):19–24
109. Ishikawa M, Kanemoto M, Morita M (1999) Control of lithium metal anode cycleability by electrolyte temperature. J Power Sources 81–82:217–220. doi:10.1016/S0378-7753(98)00213-4
110. Ishikawa M, Takaki Y, Morita M, Matsuda Y (1997) Improvement of charge-discharge cycling efficiency of li by low-temperature precycling of Li. J Electrochem Soc 144(4):L90–L92
111. Wilkinson D, Blom H, Brandt K, Wainwright D (1991) Effects of physical constraints on Li cyclability. J Power Sources 36(4):517–527